Movement of the Intermediate and Rate Determining Transition State of Barnase on the Energy Landscape with Changing Temperature

Paul A. Dalby, Mikael Oliveberg,‡ and Alan R. Fersht*

Cambridge Centre for Protein Engineering, Hills Road, Cambridge CB2 2QH, England, U.K.

Received November 14, 1997; Revised Manuscript Received January 14, 1998

ABSTRACT: Barnase folds cooperatively via an intermediate, followed by a rate-limiting transition state. We have probed possible movements of the intermediate and transition state on the energy landscape with changing temperature, from the temperature dependence of ϕ-values. These measure interaction energies at the level of individual residues. The results suggest that single destabilizing mutations can redistribute the structures in each ensemble on the energy landscape as the temperature is varied. The results were also analyzed in terms of the bulk properties of each ensemble and their movements on the energy landscape. These movements can be described in terms of the "new view" or equivalently in terms of the classical "Hammond" or "anti-Hammond" effects, observed previously for the transition states of barnase at 7.25 M urea and chymotrypsin inhibitor 2 (CI2) at 0.3 and 6 M GdmCl. The results presented here are under more relevant physiological conditions, free of chemical denaturants. The "average" structures of the intermediate and the transition state do not appear to move on the energy landscape as the temperature is varied. However, there are small rearrangements in the major α-helix of the transition state, its average structure moving closer to the native state as the temperature is increased, in agreement with the Hammond effect observed previously.

Previous studies on the folding pathway of barnase by ϕ-value analyses (*1*, *2*) have characterized extensively the folding intermediate and major transition state and have shown recently that the intermediate is formed cooperatively from the denatured state (*3*). Barnase is thus currently believed to fold according to the minimal scheme:

$$D \rightleftarrows I \rightleftarrows (\ddagger) \rightleftarrows N$$

Little is known experimentally, however, about the dynamics of these states. Analysis of the Hammond and anti-Hammond behavior of barnase at 7.25 M urea (*4*, *5*) is consistent with an ensemble of many closely spaced energy levels in the transition state. But, does the transition state move in a similar way around the energy landscape with changing conditions in the absence of chemical denaturant and, furthermore, does the intermediate consist of a similar ensemble?

Proteins have dynamic structures which rapidly sample many conformational substates around the mean structure obtained by X-ray crystallography or NMR (*6*−*10*). It is, therefore, expected that folding intermediates and transition states will have structures that may be even more dynamic. Evidence indeed suggests that this is so for folding intermediates and transition states (*11*−*14*). There is a complex dependence on temperature for the ϕ-values of formation of the intermediate and major transition state of barnase (*3*), indicating that these states are more complex than narrow discrete states.

ϕ-values are good measures of the degree of structure formed at the site of mutation in a partially formed state, relative to the fully folded state (*15*). Therefore, they can also be used as a measure of the position of the partially formed state along the reaction coordinate. At first glance, the variety of temperature dependencies for the ϕ-values observed previously throughout the structure of barnase (*3*) suggests that mutations produce movements of the intermediate and transition state along the reaction coordinate, sometimes becoming more folded and sometimes becoming less folded, irrespective of the location of the mutation. These observations do not, at first, appear to correlate with the Hammond effect observed previously for only the major α-helix in the transition state. The Hammond effect is the movement of a transition state along the reaction coordinate, becoming closer in structure to the product state, as the product is destabilized (*16, 17*). Several studies have used *m*-values (the dependence of the free energy of formation of any state on denaturant concentration) to demonstrate movements in the position of the transition state as conditions are varied. However, these Hammond or anti-Hammond effects are usually observed in high concentrations of denaturant (*4, 5, 18, 19*). Here, we present a model which accounts for the complex variations in the temperature dependence of the ϕ-values for formation of the intermediate and major transition state, which also gives an insight into the complex nature of the intermediate and transition state. We also demonstrate Hammond behavior in the transition state at physiological conditions, in full agreement with previous results at 7.25 M urea.

‡ Present address: Biochemistry, Chemical Centre, Lund University, Lund, Sweden.

S0006-2960(97)02798-0 CCC: $15.00
Published on Web 03/13/1998

EXPERIMENTAL PROCEDURES

Temperature Dependence of ϕ-Values. The temperature dependence of the ϕ-values for the formation of the intermediate from the denatured state (ϕ_{I-D}) and the formation of the transition state from the denatured state ($\phi_{\ddagger-D}$) were obtained in 50 mM MES (19.4 mM acid form and 30.6 mM sodium salt), pH 6.3, in the 15−50 °C range, as published previously, according to eqs 1 and 2 (*3*).

$$\phi_{\ddagger-D} = \left(\frac{\Delta\Delta G_{\ddagger-D}}{\Delta\Delta G_{N-D}}\right) \quad (1)$$

$$\phi_{I-D} = \left(\frac{\Delta\Delta G_{I-D}}{\Delta\Delta G_{N-D}}\right) \quad (2)$$

Temperature Dependence of $\Delta G_{\ddagger-N}$.[1] The temperature dependence of the free energy of formation of the transition state from the native state, $\Delta G_{\ddagger-N}$, was obtained for each mutant, from the temperature dependence of the unfolding rate constant (k_u), according to eq 3. The temperature dependence of k_u for wild type and mutants of barnase have been published previously (Dalby et al., 1997). From transition state theory,

$$\Delta G_{\ddagger-N} = RT\ln(A) - RT\ln(k_u) \quad (3)$$

where the constant $A = \kappa k_B T/h$, k_B is the Boltzmann constant, h is the Planck constant, κ is a transmission constant (assumed to be unity for convenience), and T is the temperature in kelvin.

RESULTS

Temperature Dependence of ϕ-Values. The temperature dependence of the ϕ-values for the formation of the intermediate from the denatured state (ϕ_{I-D}) and the formation of the transition state from the denatured state ($\phi_{\ddagger-D}$), in the 15−50 °C range, have been published previously for all 16 destabilizing mutants studied in 50 mM MES (19.4 mM acid form and 30.6 mM sodium salt), pH 6.3 (*3*). The mutants are listed and described in Table 1. The mutations are distributed throughout the N-terminal region, α-helix$_1$, loop$_2$, α-helix$_3$, loop$_3$, β-sheet, and hydrophobic core$_1$, with a bias toward α-helix$_1$. Figures 1 and 2 show examples of various types of temperature dependence observed for ϕ_{I-D} and $\phi_{\ddagger-D}$, respectively. Data above 33 °C are not shown for ϕ_{I-D} since the plots often deviate above this temperature (*3*). Both temperature dependencies vary from strong positive gradients, through zero, to strong negative gradients. The slopes ($\partial\phi/\partial T$) of these plots at 25 °C are shown in Table 1, along with the actual ϕ-values at 25 °C for reference. The slopes were obtained by fitting the plots of ϕ vs T to second or third-order polynomial equations (eqs 4 and 5, respectively). The slopes at any temperature were then obtained from the derivatives of these equations (eqs 6 and 7, respectively).

Table 1: ϕ-Values for the Formation of the Intermediate and the Transition State and Their Temperature Dependence at 25 °C

mutant	location	ϕ_{I-D}[a]	$\phi_{\ddagger-D}$[b]	$\partial\phi_{I-D}/\partial T$[c] °C^{-1}	$\partial\phi_{\ddagger-D}/\partial T$[c] °C^{-1}
IA4	N-terminus	−0.08	−0.04	0.0061	0.0086
TG6	helix$_1$ N-cap	0.06	0.08	0.0081	0.0097
DA8	helix$_1$	0.41	0.64	−0.0188	−0.0182
DG8	helix$_1$	0.69	0.80	−0.0031	−0.0036
AG8	helix$_1$	1.06	1.03	0.0238	0.0203
DG12	helix$_1$	0.35	0.50	−0.0013	0.0031
YA17	helix$_1$	0.35	0.50	−0.0027	−0.0002
HN18	helix$_1$	0.58	0.71	0.0001	0.0013
VA36	loop$_2$	0.39	0.38	−0.0141	−0.0141
NA41	helix$_3$ N-cap	0.19	0.19	−0.0151	−0.0142
NA58	loop$_3$	0.96	0.97	−0.0060	−0.0057
IV88	β_3, core$_1$	0.49	0.73	−0.0020	0.0037
SA91	β-strand$_3$	0.72	0.98	−0.0027	0.0005
SA92	β-turn	0.57	0.58	−0.0142	−0.0136
IV96	β_4, core$_1$	0.45	0.46	0.0192	0.0200
TV105	loop$_5$	0.18	0.36	0.0034	0.0074

[a] ϕ-value for the formation of the intermediate from the denatured state at 25 °C. [b] ϕ-value for the formation of the transition state from the denatured state at 25 °C. A ϕ-value of 0 corresponds to a state which is as unstructured as the denatured state at the point of mutation. A ϕ-value of 1 corresponds to a state which is as structured as the native state at the point of mutation. [c] Slope of the temperature dependence of each ϕ-value, obtained by fitting the temperature dependence to a second- or third-order polynomial, then calculating the derivative at 25 °C (see Experimental Methods). All data are at 25 °C in 50 mM MES, pH 6.3.

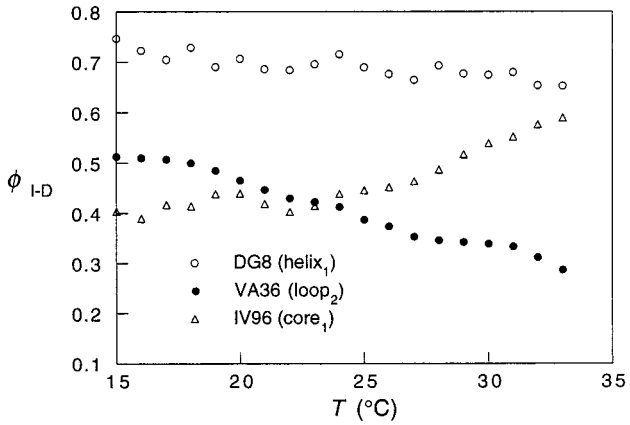

FIGURE 1: Temperature dependence of the ϕ-value for the formation of the intermediate from the denatured state, for the three mutants (○) DG8, (●) VA36, and (△) IV96, demonstrating the variations observed.

$$\phi = m_1 + m_2T + m_3T^2 \quad (4)$$

$$\phi = m_1 + m_2T + m_3T^2 + m_4T^3 \quad (5)$$

$$\partial\phi/\partial T = m_2 + 2m_3T \quad (6)$$

$$\partial\phi/\partial T = m_2 + 2m_3T + 3m_4T^2 \quad (7)$$

Figures 3 and 4 show how the slopes are distributed for the temperature dependencies of ϕ_{I-D} and $\phi_{\ddagger-D}$, respectively. The slopes vary through the whole range of −0.02 to 0.02 (°C^{-1}), but slopes closer to zero appear to be more frequent.

[1] Abbreviations: GdmCl, guanidinium chloride; CI2, chymotrypsin inhibitor 2; ΔG, change in free energy; LFER, linear free energy relationship.

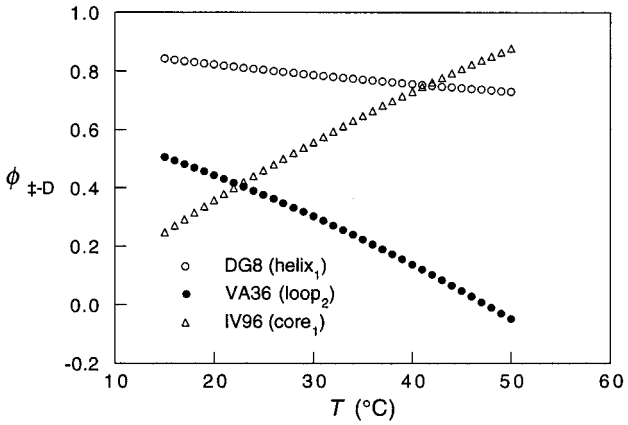

FIGURE 2: Temperature dependence of the ϕ-value for the formation of the transition state from the denatured state, for the three mutants (○) DG8, (●) VA36, and (△) IV96, demonstrating the variations observed.

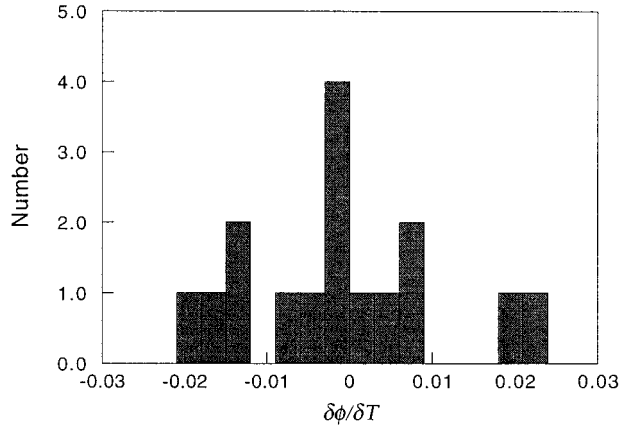

FIGURE 3: Distribution of slopes ($\partial\phi_{I-D}/\partial T$), for the temperature dependence of ϕ_{I-D}, the ϕ-value for the formation of the intermediate from the denatured state. The average slope is close to zero, indicating that on average the intermediate maintains a constant degree of structure formation. The distribution of slopes indicates a variety of structural rearrangements for different mutants.

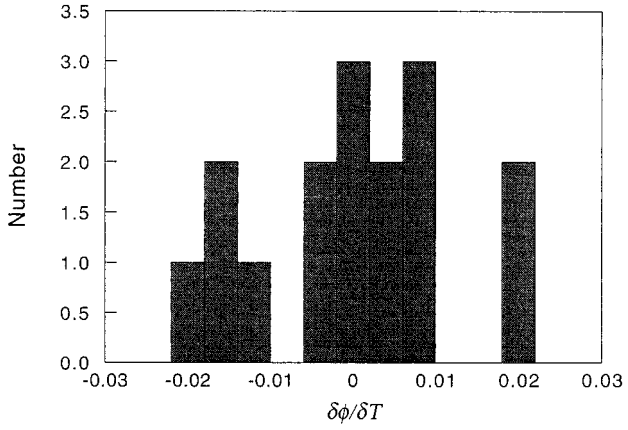

FIGURE 4: Distribution of slopes ($\partial\phi_{‡-D}/\partial T$), for the temperature dependence of $\phi_{‡-D}$, the ϕ-value for the formation of the transition state from the denatured state. The average slope is greater than zero, indicating that on average the transition state becomes more structured with increasing temperature. The distribution of slopes indicates a variety of structural rearrangements for different mutants.

Temperature Dependence of Averaged ϕ-Values. The temperature dependencies of the average values of ϕ_{I-D} and $\phi_{‡-D}$, for the whole protein, helix$_1$ only, and residues not in helix$_1$, are shown in Figures 5 and 6, respectively. The whole protein values are averaged from all 16 mutants. The helix$_1$ values are averaged from the six mutants DA8, DG8, AG8, DG12, YA17, and HN18.

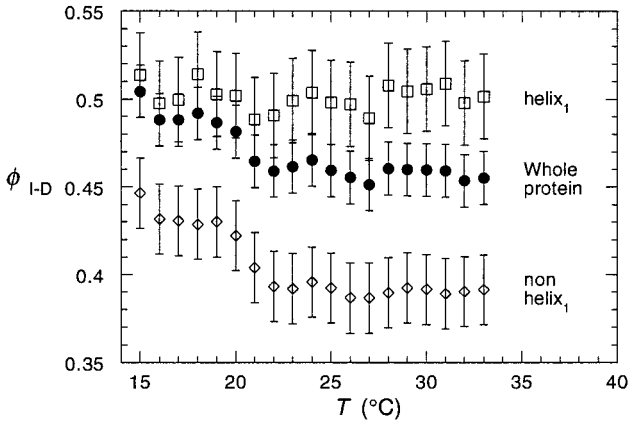

FIGURE 5: Temperature dependence of the average ϕ-values of formation of the intermediate from the denatured state (ϕ_{I-D}), from (○) the whole protein, (□) helix$_1$ only and (◇) nonhelix$_1$ residues.

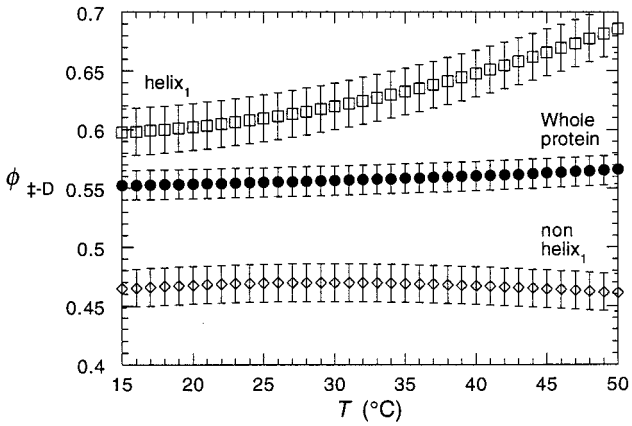

FIGURE 6: Temperature dependence of the average ϕ-values of formation of the transition state from the denatured state ($\phi_{‡-D}$), from (○) the whole protein, (□) helix$_1$ only and (◇) nonhelix$_1$ residues.

The average value of ϕ_{I-D} for helix$_1$ is independent of temperature and has a value of approximately 0.5. However, the average value of ϕ_{I-D} for nonhelix$_1$ mutants, and subsequently to a lesser extent for the whole protein, is independent of temperature except for a slight decrease between 19 and 22 °C from a value of 0.43 to 0.39. It is difficult to determine, however, whether this decrease is significant or not, due to errors of a similar magnitude. The implication of these data, therefore, is that the average structure of the intermediate does not move along the reaction coordinate as the temperature is varied, although from the distribution of slopes above, an interaction at any particular residue may become more or less structured as the temperature changes.

The average values of $\phi_{‡-D}$ for the whole protein, and for nonhelix$_1$ mutants, are virtually independent of temperature and have values of approximately 0.55 and 0.46, respectively. Helix$_1$, however, shows an increase in $\phi_{‡-D}$ with increasing temperature, becoming more rapid as the temperature is increased. Therefore, these data imply the same variations of structure on average and at the residue level, except that there is an indication of Hammond behavior in helix$_1$; *i.e.*, the transition state becomes more similar to the native state

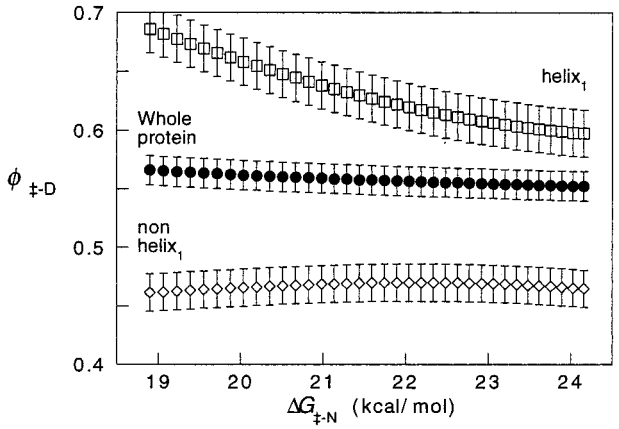

FIGURE 7: Hammond plot for the transition state, where the ϕ-value of formation of the transition state from the denatured state ($\phi_{\ddagger-D}$) is a measure of the position of the transition state along the reaction coordinate, relative to the native state. The average transition-state structure of helix$_1$ (□) clearly demonstrates Hammond behavior since it becomes more nativelike as the transition state becomes closer in energy to the native state. The average transition-state structures for the whole protein (●) and the nonhelix$_1$ regions (◇) do not show any significant Hammond behavior.

as conditions become more destabilizing.

Hammond Behavior in Helix$_1$ of the Transition State. Hammond behavior is defined by a transition state becoming closer in energy to the product (native) state and also becoming more similar in structure (*16*). $\Delta G_{\ddagger-N}$ has been calculated by using eq 3 (see Experimental Procedures), where A ($=\kappa k_B T/h$), is usually of the order of 6×10^{12} s^{-1}, at 298 K. A may be quantitatively wrong for proteins, since transition state theory applies to simple small molecules. However, the errors in A would be the same for all mutants of a protein and so would not affect the qualitative results described here. Figure 7 shows a plot of the averaged values of $\phi_{\ddagger-D}$ vs $\Delta G_{\ddagger-N}$, for the whole protein, helix$_1$ only, and nonhelix$_1$ mutations. It is important to note that the average free energy for helix$_1$ mutants differs only by a constant 0.4 kcal mol^{-1}. These Hammond plots confirm that Hammond behavior is observed, on average, for helix$_1$ only.

DISCUSSION

Linear free energy relationships (LFERs) relate the free energy of formation of an intermediate or transition state to that of the product state. They are a useful method for measuring the position of a partially formed state along the reaction coordinate for protein folding. A commonly used LFER is $\beta_T = (m_{\ddagger-N}/m_{D-N})$, obtained from the denaturant concentration dependencies of the corresponding free energies (*4*, *20*). This method measures the degree of solvation of a state, relative to that of the product (*21*). ϕ-values are another useful LFER. Unlike β_T, they measure the position of a state along the reaction coordinate, using a single residue as the probe. For a partially formed state, **X**, $\phi_{X-D} = \Delta\Delta G_{X-D}/\Delta\Delta G_{N-D}$ (see eqs 1 and 2 in Experimental Procedures). Thus, in the folding direction, a ϕ-value of 1 corresponds to a partially formed state which is as structured at the point of mutation, as the native state. A ϕ-value of 0 corresponds to a partially formed state which is as unstructured at the point of mutation, as the denatured state. A ϕ-value between 0 and 1 is more complicated, however, since it could correspond to a partially formed structure at the point of mutation, but it could also correspond to a population of states with varying amounts of structure at the point of mutation, whose average ϕ-value is between 0 and 1 (*22*).

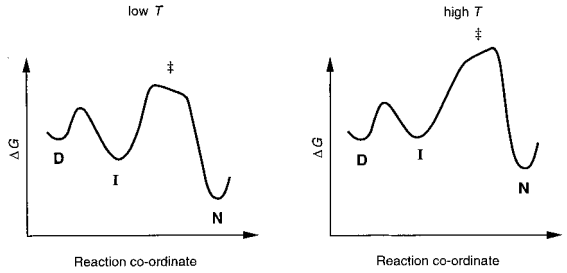

FIGURE 8: Effect of increasing the temperature on the free energy landscape for folding. The more structured states in the transition-state ensemble destabilize more than the less structured states. The highest point in the transition-state ensemble moves toward the native state on the reaction coordinate as the temperature is increased, producing a Hammond effect.

Apart from the position of a state on the reaction coordinate, ϕ-values are affected by second-order effects, termed structure−reactivity relationships (*17*, *5*). One of these affects, the Hammond effect (*16*), is the movement of a transition state on the energy landscape, along the reaction coordinate, becoming closer in structure to the product state as the product is destabilized. Lesser known is the anti-Hammond effect, in which the transition state moves perpendicular to the reaction coordinate on the energy landscape, such that its structure becomes less productlike in certain regions, as the product is destabilized, even though the average structure may still exhibit Hammond behavior.

Examples of how the ϕ-values for the formation of the intermediate (ϕ_{I-D}), and the major transition state ($\phi_{\ddagger-D}$) vary with temperature are shown in Figures 1 and 2, respectively. It can be seen that the ϕ-values change smoothly with temperature, showing no sudden deviations. Data above 33 °C have been excluded for ϕ_{I-D}, as deviations often occur above this temperature, as a result of the population of a second intermediate (*3*). These smooth temperature dependencies are likely to be due to gradual changes in the energy landscape for folding, as the temperature is varied.

The distributions of all of the observed temperature dependencies, as determined by their slopes ($\partial\phi/\partial T$), at 25 °C, are shown in Figures 3 and 4, for the intermediate and the transition state, respectively. It is clearly noticeable from Figure 3 that the distribution of slopes for the intermediate is quite symmetrical, with more of the slopes being closer to zero than at the extremes of ± 0.02 °C^{-1}. The distribution of slopes for the transition state, however, is slightly less symmetrical, although again most of the slopes are closer to zero than at the extremes of ± 0.02 °C^{-1}.

The above data can be explained by the so-called "new view" in terms of a redistribution of the funnel-shaped energy landscape with changing temperature (*23*), which is equivalent to the classical model of Hammond and anti-Hammond effects. The Hammond behavior observed for α-helix$_1$ of the transition state is readily explained by invoking a simple free energy reaction coordinate. Figure 8 shows schematically how we expect the reaction coordinate for the folding of barnase to change as the temperature is increased. The transition state is depicted as a broad maximum, indicating that it is comprised of an ensemble of states with varying degrees of structure formed.

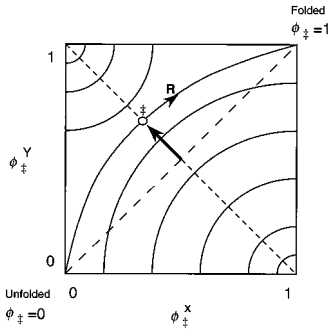

FIGURE 9: Movement (bold arrow) of the transition-state saddle point (circle) on the folding energy landscape as the temperature is increased, producing an anti-Hammond effect at residue X and a Hammond effect at residue Y. The average degree of structure remains constant. The contours indicate structures of increasing energy, as the contour radii decrease. The large dashes represent the reaction coordinate and the smaller dashes represent the transition state boundary. R indicates the lowest energy reaction pathway.

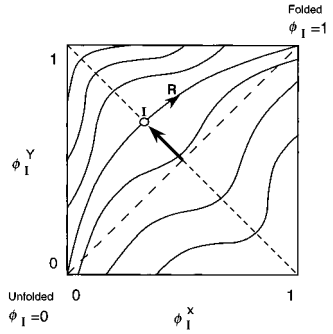

FIGURE 10: Movement (bold arrow) of the intermediate energy minimum (circle) on the folding energy landscape as the temperature is increased, producing an "apparent" anti-Hammond effect at residue X and an "apparent" Hammond effect at residue Y. The average degree of structure remains constant. The contours indicate structures of increasing energy. The large dashes represent the reaction coordinate and the smaller dashes represent the ensemble of states with the same average degree of structure. R indicates the lowest energy reaction pathway.

The changes with temperature in the average free energies of the intermediate, transition state, and native state relative to the denatured state have been characterized previously (*24*). Figure 8 shows these changes, with the expected effects of temperature on the transition-state ensemble, superimposed. We assume that the more structured species in the ensemble, *i.e.*, those further along the reaction coordinate, destabilize more rapidly as the temperature is increased than the less structured species. The result is that the maximum in the transition-state ensemble becomes more structured on destabilization of both the native and transition states, which is the Hammond effect.

The effect of temperature on the ϕ-values from individual mutations, for formation of the transition state and intermediate, requires a more complex explanation. Rearrangements of structure within an ensemble, due to changing temperature, could possibly involve a series of complementary effects, whereby an increase in structure at one set of residues has an accompanying set of residues for which the structure is weakened, thus maintaining a similar global free energy. The transition state for any reaction can be represented by a saddle point on the free energy landscape, with higher energy transition states on either side, perpendicular to the reaction coordinate, and lower energy states on either side, along the reaction coordinate (Figure 9). Figure 9 shows the effect of increasing the temperature on the energy landscape, in a region of the transition state which does not exhibit Hammond behavior. The transition-state saddle point moves perpendicular to the reaction coordinate, resulting in a decrease in structure at residue "X" and a complementary increase in structure at residue "Y". The overall result is a decrease in $\phi_{\ddagger-D}$ for mutant X, as the temperature is increased, *i.e.*, anti-Hammond behavior, and an increase in $\phi_{\ddagger-D}$ for mutant Y, i.e., Hammond behavior. The average value of $\phi_{\ddagger-D}$, however, remains independent of temperature. The energy landscape minimum for the folding intermediate can be described by the same behavior (Figure 10). Here, the changing temperature moves the minimum of the intermediate perpendicular to the reaction coordinate, producing the same decreases and increases in ϕ_{I-D} for different mutants. The average value of ϕ_{I-D} also remains independent of temperature.

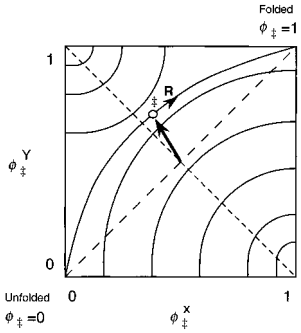

FIGURE 11: Movement (bold arrow) of the transition-state saddle point (circle) on the folding energy landscape as the temperature is increased, producing an anti-Hammond effect at residue X and a Hammond effect at residue Y, as before. The average ensemble becomes more structured and moves along the reaction coordinate toward the native state. The contours indicate structures of increasing energy, as the contour radii decrease. The large dashes represent the reaction coordinate and the smaller dashes represent the initial transition state boundary. R indicates the lowest energy reaction pathway.

The distributions of the slopes of ϕ vs T, for both the intermediate and the transition state (Figures 3 and 4), show that slopes closer to zero are more frequent. This implies that the variation in ϕ-values within each ensemble is most frequently small. Therefore, in dynamic terms, both the intermediate and transition state can be defined mainly by a core of relatively fixed interactions, surrounded by regions of fluctuating structure and then regions of no defined structure.

To measure movements of the whole intermediate and transition-state ensembles along the reaction coordinate, the ϕ-values for all 16 mutants were averaged together to give the average temperature dependencies of ϕ_{I-D} and $\phi_{\ddagger-D}$ respectively in Figures 5 and 6. Also shown are the averages for the six α-helix$_1$ residues and for the remaining 10 residues. It is clear from Figure 5 that the intermediate ensemble, on the whole, does not move along the reaction coordinate as the temperature is increased, although there is a slight weakening of structure at 19−22 °C. The average structure of α-helix$_1$ also remains unperturbed by temperature. The slight weakening of structure at 19−22 °C is attributable, therefore, to regions of the protein not in

α-helix$_1$. However, it is still difficult to determine whether this weakening is significant or not, due to errors of a similar magnitude.

From Figure 6, it is clear that the transition-state ensemble, on average, does not move along the reaction coordinate as the temperature is increased. However, the average structure of α-helix$_1$ becomes more structured as the temperature is increased; *i.e.*, it moves closer to the native state on the reaction coordinate. The remaining structure on average is unperturbed by temperature. To confirm that this change in structure is in fact Hammond behavior, the same averages of $\phi_{\ddagger-D}$ are plotted against the average $\Delta G_{\ddagger-N}$ for the whole protein (Figure 7). As discussed above, $\Delta G_{\ddagger-N}$ for α-helix$_1$ only differs only by a constant 0.4 kcal mol^{-1} from $\Delta G_{\ddagger-N}$ for the whole protein, and so both provide a suitable index for testing Hammond behavior in both the whole protein and α-helix$_1$ only. Figure 7 shows that for α-helix$_1$ only, as $\Delta G_{\ddagger-N}$ decreases, $\phi_{\ddagger-D}$ increases from 0.6 to 0.7. In other words, as the difference in free energy between the transition state and the native state decreases, they become more similar in structure. This is the Hammond behavior observed previously for barnase in 7.25 M urea (*4*, *5*, *18*).

The Hammond behavior observed for α-helix$_1$ can also be incorporated into the energy landscapes described above (Figure 11). Here, the same movements of the transition state along the reaction coordinate, shown in Figure 8, produce a movement along the reaction coordinate on the energy landscape. In Figure 11, the bold arrow represents the movement of the transition state on the energy surface as the temperature is increased. Now, the result is a decrease in $\phi_{\ddagger-D}$ for mutant X as the temperature is increased, i.e., anti-Hammond behavior, and an increase in $\phi_{\ddagger-D}$ for mutant Y, i.e., Hammond behavior, but the average value of $\phi_{\ddagger-D}$, however, also increases with temperature, i.e., Hammond behavior.

Previous studies strongly implied Hammond behavior in the transition state for the main hydrophobic core, as well as clear Hammond behavior for α-helix$_1$ (*4*). The present study, however, can only be used to show Hammond behavior in α-helix$_1$, since the mutations are biased toward probing the helix and then the rest of the protein as a whole.

The current results are consistent with the previous results for Hammond and anti-Hammond behavior in barnase, which suggested that the transition state consists of an ensemble of states with closely spaced energy levels and also that α-helix$_1$ plays an important role in the rate determining step, probably due to the hydrophobic face of the helix forming a major part of the hydrophobic core. The present results, however, also suggest that the intermediate consists of a similar ensemble of closely spaced energy levels. They also suggest that the average structure of the intermediate does not move significantly along the reaction coordinate with changing temperature since there is no "apparent" Hammond effect. It should be noted that any movement of an intermediate along the reaction coordinate cannot strictly be described by the Hammond effect, a term that applies only to transition states.

CONCLUSIONS

Individual mutations produce a whole range of dependencies of ϕ-values on temperature, for both the intermediate and the transition state at physiological conditions. These variations can be explained in terms of apparent Hammond and anti-Hammond behavior as the two states move perpendicular to the reaction coordinate on the energy landscape. Both of these states contain a core group of residues whose structure fluctuates very little and then progressively smaller sets of residues which fluctuate between two increasingly large extremes of structure formation. The average structure of the intermediate remains unperturbed by changes in temperature, as does, on average, most of the transition-state structure. The major α-helix in the transition state, however, displays Hammond behavior, consistent with previous observations at 7.25 M urea. The temperature independence of much of the structure lends to the validity of comparing computer simulations of unfolding at high temperature with experimental data at lower temperatures (*25*).

REFERENCES

1. Matouschek, A., Serrano, L., and Fersht, A. R. (1992) *J. Mol. Biol. 224,* 819−835.
2. Serrano, L., Matouschek, A., and Fersht, A. R. (1992) *J. Mol. Biol. 224,* 805−818.
3. Dalby, P. A., Oliveberg, M., and Fersht, A. R. (1998) *J. Mol. Biol.*, in press.
4. Matouschek, A., and Fersht, A. R. (1993) *Proc. Natl. Acad. Sci. U.S.A.* 90, 7814−7818.
5. Matthews, J. M., and Fersht, A. R. (1995) *Biochemistry 34,* 6805−6814.
6. Linderstrøm-Lang, K. (1955) *Chem. Soc. (London), Spec. Publ. 2,* 1−20.
7. Karplus, M., and McCammon, J. A. (1983) *Annu. Rev. Biochem. 53,* 263−300.
8. Wagner, G. (1983) *Quart. Rev. Biophys. 16,* 1−57.
9. Englander, S. W., and Kallenbach, N. R. (1984) *Quart. Rev. Biophys. 16,* 521−655.
10. Frauenfelder, H., Parak, F., and Young, R. D. (1988) *Annu. Rev. Biophys. Biophys. Chem 17,* 451−479.
11. Jones, B. E., Beechem, J. M., and Matthews, C. R. (1995) *Biochemistry 34,* 1867−1877.
12. Ptitsyn, O. B. (1995) *Curr. Opin. Struct. Biol. 5,* 74−78.
13. Parker, M. J., Sessions, R. B., Badcoe, I. G., and Clarke, A. R. (1996) *Folding & Design 1,* 145−156.
14. Silow, M., and Oliveberg, M. (1997) *Biochemistry 36,* 7633−7637.
15. Fersht, A. R., Matouschek, A., and Serrano, L. (1992) *J. Mol. Biol. 224,* 771−782.
16. Hammond, G. S. (1955) *J. Am. Chem. Soc. 77,* 334−338.
17. Jencks, W. P. (1985) *Chem. Rev. 85,* 511−527.
18. Matouschek, A., Otzen, D. E., Itzhaki, L. S., Jackson, S. E., and Fersht, A. R. (1995) *Biochemistry 34,* 13656−13662.
19. Ibarra-Molero, B., and Sanchez-Ruiz, J. M. (1996) *Biochemistry 35,* 14689−14702.
20. Parker, M. J., Spencer, J., and Clarke, A. R. (1995) *J. Mol. Biol. 253,* 771−786.
21. Schellman, J. A. (1978) *Biopolymers 17,* 1305−1322.
22. Fersht, A. R. (1993) *FEBS Lett. 325,* 5−16.
23. Bryngelson, J. D., Onuchic, J. N., Socci, N. D., and Wolynes, P. G. (1995) *Proteins: Struct. Funct. Genet. 21,* 167−195.
24. Oliveberg, M., and Fersht, A. R. (1996) *Biochemistry 35,* 2738−2749.
25. Bond, C. J., Wong, K.-B., Clarke, J., Fersht, A. R., and Daggett, V. (1997) *Proc. Natl. Acad. Sci. U.S.A. 94,* 13409−13413.

BI972798D